

Proton diffusion in noble metals

Satya Prakash*

*Equipe de Recherche No. 81 du Centre National de la Recherche Scientifique, Université Paris XI,
Bâtiment 350, 91405 Orsay, France*

(Received 14 March 1977)

The configurational and activation energies of proton are investigated in noble metals within the framework of many-particle theory. Model pseudopotentials are used to represent the bare ions of the host lattice and the modified Hartree dielectric function which includes the exchange-correlation corrections explicitly, is used for the screening due to conduction electrons. The octahedral position is found to be more stable for the proton, but this is most likely to be trapped into a vacancy if available. The activation energies are found to be in reasonably good agreement with the experimental values for effective proton charges $0.31e$, $0.29e$, and $0.23e$ in copper, silver, and gold, respectively. The configurational and activation energies are found to decrease as the lattice is expanded.

I. INTRODUCTION

There has recently been an upsurge of interest in the interaction of hydrogen with metals. This is because of both the practical utility of metal-hydrogen alloys and availability of more sophisticated techniques to study the pure metals of interest. There is a greater deal of experimental data for diffusion of hydrogen in metals and these have been interpreted using classical rate theory^{1,2} (a good amount of information can be obtained from Refs. 1 and 2 and the references given in the papers therein). However a satisfactory explanation on the basis of microscopic theory is still awaited. Friedel³ was the pioneer in making a quantum-mechanical investigation of the electronic distribution around the hydrogen dissolved in monovalent copper metal and estimating the heat of solution using Thomas-Fermi (TF) screening self-consistently. Friedel pointed out that the proton may be screened by the Fermi gas and under certain conditions this screening may also occur through the formation of bound states below the bottom of the Fermi distribution. These calculations were further extended by Leonard⁴ in the linearized self-consistent Hartree approximation to estimate the residual resistivity of CuH. The estimated results of these authors agree reasonably with experiments. Popovic *et al.*^{5,6} formulated the pseudopotential theory for heat of solution and diffusion of hydrogen in simple metals. These authors treated the electronic contribution to the heat of solution in the framework of a local pseudopotential and linear screening while for the proton contribution they emphasized the use of nonlinear screening as done by Carbotte⁷ for positron screening. Their results for the heat of solution and activation energy are in good agreement with the experiment for Al, but for Mg no conclusion could be drawn. Gelatt *et al.*⁸ calculated the

heat of formation of $3d$ and $4d$ transition-metal hydrides, and they found that it is not directly related to the Fermi-level density of states, which is in contrast to the prediction of the screened-proton model.

Flynn and Stoneham⁹ developed quantum theory of diffusion for light interstitials with an emphasis on transitions among localized states and these authors discussed the diffusion in bcc and fcc lattices. Stoneham¹⁰ further discussed the temperature dependence of the diffusion rate. Mainwood and Stoneham¹¹ investigated the diffusion of H in liquid and solid metals using cluster calculations. Recently, Birnbaum and Flynn¹² gave a consistent interpretation of low temperature properties of H and D in Nb in terms of a system of tunnel split pocket states. Lepski¹³ and Gorham-Bergeron¹⁴ developed the dynamical theory of hydrogen diffusion in metals using the Kubo formula, and explained the lattice-hydrogen interaction and mass dependence of activation energy. However, all these theories are still qualitative and detailed calculations are awaited.

Friedel pointed out that in copper, the screening of a proton by conduction electrons is more probable than by core electrons, the additional charge being near the bottom of the conduction band. Thus assuming the absence of bound states, Gubanov and Nikulin¹⁵ developed the theory of configurational energy of proton in the framework of many-particle theory using a linear screening approximation, and applied it to noble metals. They used the model pseudopotential for the bare ions of the host lattice and TF screening function. Since then, many reliable model potentials have become available which explain many of the physical properties in solid and liquid phases of these metals. The modified Hartree (MH) dielectric function, where exchange and correlation corrections are included satisfactorily, is also available. Therefore, with

the present state of understanding of proton diffusion in these metals, we found it interesting to extend this approach for detailed investigations. Although this approach is more suitable for simple metals, a little experimental information is available for these metals. Among noble metals, Ag is more like a simple metal since the filled d band is sufficiently narrow and well below the Fermi energy. The filled broad d band in the conduction band does affect the physical properties of noble metals, but this effect has indirectly been included in the determination of the model potential parameters as these are obtained by fitting to some experimental results.

The plan of the paper is as follows: the necessary formalism is presented in Sec. II, the results and discussions are presented in Sec. III, and these are concluded in Sec. IV.

II. THEORY

Following the approach of Gubanov and Nikulin,¹⁵ a system of electrons and ions forming the lattice framework and the proton introduced in it, is considered. The Hamiltonian for such a system is

$$H = H_0 + ZV,$$

where H_0 is the Hamiltonian of the perfect crystal of stationary ions and ZV is the interaction strength of the proton with the lattice. Ze is the effective charge of the proton, and Z is regarded as a switching on parameter. If $\phi(Z)$ is the state vector of the perturbed system, the energy of introduction of proton can be written

$$\Delta E^i(\vec{R}) = E - E_0 = \int_0^Z dZ \langle \phi(Z) | V(\vec{R}) | \phi(Z) \rangle, \quad (2)$$

where E and E_0 are the expectation values of H and H_0 , respectively. \vec{R} is the position vector of the proton. If we restrict $\Delta E^i(\vec{R})$ to lowest order and use the linear screening approximation to calculate the ionic densities, the simplified expression obtained for the configurational energy of the proton, is

$$\Delta E(\vec{R}) = 4\pi Ze^2 \int \frac{d\vec{q}}{(2\pi)^3} \left[\rho_i(\vec{q}) - \frac{V_L(\vec{q})q^2}{4\pi} \left(1 - \frac{1}{\epsilon_0(\vec{q})} \right) \right] \times (1/q^2) e^{i\vec{q} \cdot \vec{R}}. \quad (3)$$

$\rho_i(\vec{q})$ is the Fourier transform of ionic density given as $\rho_i(\vec{r}) = Z_i \sum_l \delta(\vec{r} - \vec{R}_l)$, where Z_i is the ionicity of the l th ion at \vec{R}_l . $V_L(\vec{q}) = \sum_l \exp(i\vec{q} \cdot \vec{R}_l) v(\vec{q})$, where $v(\vec{q})$ is the unscreened form factor normalized in unit volume. $\epsilon_0(\vec{q})$ is the MH dielectric function given as

$$\epsilon_0(\vec{q}) = 1 + [1 - f(\vec{q})] (2k_F/\pi q^2) \times \left(1 + \frac{4k_F^2 - q^2}{4k_F q} \ln \left| \frac{2k_F + q}{2k_F - q} \right| \right), \quad (4)$$

where k_F is Fermi momentum and $f(\vec{q})$ is a Vashishta and Singwi¹⁶ Gaussian function for exchange-correlation corrections. In the derivation of Eq. (3), the lattice-distortion effects³ and the local-field corrections are also neglected.¹⁷

The accuracy of the configurational energy calculations depends upon the suitable choice of the model potential and the dielectric function. We choose the following four model potentials whose parameters are determined with the help of some experimental data rather than *a priori*.

(a) Nikulin model potential (H): Nikulin¹⁸ defined a Heine-Abarenkov-type model potential

$$V_H(r) = -A\Theta(\vec{r}_0 - \vec{r}) - (Z_1/r)\Theta(\vec{r} - \vec{r}_0), \quad (5)$$

where $\Theta(x)$ is the step function. The parameters A and r_0 are determined by fitting the optical term values.

(b) Ashcroft model potential (A): This is the same as Eq. (5) with $A = 0$. the single parameter r_0 is determined by Ashcroft and Langreth¹⁹ with the help of liquid resistivity data.

(c) Borchi and De Gennaro potential²⁰ (B): These authors developed the model potential on intuitive physical grounds. The self-explained analytical form of the potential is

$$V_B(r) = \begin{cases} V_0 & \text{for } 0 < r < r_1, \\ -A & \text{for } r_1 < r < r_2, \\ -Z_1/r & \text{for } r > r_2. \end{cases} \quad (6)$$

The parameters V_0 , A , and r_2 are determined with the help of liquid resistivity and band-gap data, and r_1 is taken equal to Bohr radius.

(d) Singh and Prakash potential (S).¹⁷ These authors assumed a modified form of the point-ion model potential

$$V_S(r) = Ae^{-r/r_0} - Z_1/r, \quad (7)$$

and determined the parameters A and r_0 by fitting the phonon spectrum.

All these potentials are Coulombic beyond a certain distance, but below it they are different in nature. Nikulin's potential is attractive. In the Ashcroft potential, the attractive and repulsive parts mutually cancel. The Borchi *et al.* potential consists of both the attractive and repulsive parts, and the Singh *et al.* potential is damped repulsive. Therefore, the effective core size for all these potentials is different and this effect may be reflected in the calculated configurational energies. Nikulin's²¹ potential reproduces the phonon spectrum and cohesive energy in reasonable agreement

with experiments, and is also used to estimate the activation energy of protons in noble metals.¹⁵ Borchi *et al*, and Singh *et al*. potentials, respectively, reproduce the magnetic susceptibility²² and band gap¹⁷ well.

The form factors for all these potentials may readily be obtained and are used in conjunction with the MH dielectric function to obtain the expressions for the configurational energy as follows:

$$\Delta E_H(\vec{R}) = \frac{2Ze^2}{\pi} \sum_i \frac{1}{|\vec{r}_i|} \left(\frac{\pi Z_i}{2} - (Z_i - Ar_0) \int dq X(q) \frac{\cos qr_0 \sin qr_1}{q} - A \int dq X(q) \frac{\sin qr_0 \sin qr_1}{q^2} \right), \quad (8)$$

$$\Delta E_B(\vec{R}) = \frac{2Ze^2}{\pi} \sum_i \frac{1}{|\vec{r}_i|} \left(\frac{\pi Z_i}{2} - (Z_i - Ar_2) \int dq X(q) \frac{\sin qr_1 \cos qr_2}{q} - A \int dq X(q) \frac{\sin qr_1 \sin qr_2}{q^2} \right. \\ \left. + (A + V_0) \int dq X(q) \frac{\sin qr_1 \sin qr_1}{q^2} - (A + V_0)r_1 \int dq X(q) \frac{\sin qr_1 \cos qr_1}{q} \right), \quad (9)$$

$$\Delta E_S(\vec{R}) = \frac{2Ze^2}{\pi} \sum_i \frac{1}{|\vec{r}_i|} \left(\frac{\pi Z_i}{2} - Z_i \int dq X(q) \frac{\sin qr_1}{q} + \frac{A}{4\pi} \int dq X(q) \frac{q \sin qr_1}{(1 + q^2 r_0^2)^2} \right), \quad (10)$$

where

$$X(q) = 1 - \frac{1}{\epsilon_0(q)},$$

and

$$\vec{r}_i = \vec{R}_i - \vec{R}.$$

The subscripts *H*, *B*, and *S* have the same explanation as for model potentials. The expression for $\Delta E_A(\vec{R})$ may be obtained from Eq. (8) putting $A = 0$. Equations (8)–(10) may further be simplified by substituting $X(q)$, but the present form is more suitable for numerical integration over q .

The corresponding expressions in Thomas-Fermi screening limit are

$$\Delta E_{HT}(\vec{R}) = Z \sum_i \frac{\exp(-\beta r_i)}{|\vec{r}_i|} \left((Z_i - Ar_0) \cosh \beta r_0 + \frac{A}{\beta} \sinh \beta r_0 \right), \quad (11)$$

$$\Delta E_{BT}(\vec{R}) = Z \sum_i \frac{e^{-\beta |\vec{r}_i|}}{|\vec{r}_i|} \left[(Z_i - Ar_2) \cosh \beta r_2 + \frac{A}{\beta} \sinh \beta r_2 + (A + V_0)r_1 \cosh(\beta r_1) + \left(\frac{A + V_0}{\beta} \right) \sinh \beta r_1 \right], \quad (12)$$

and

$$\Delta E_{ST}(\vec{R}) = \frac{Z}{2(\beta^2 - b^2)^2} \sum_i \frac{1}{|\vec{r}_i|} \{ 2[(\beta^2 - b^2)Z_i + \alpha b^4 \beta^2] e^{-\beta r_i} + \alpha \beta^2 b^3 (\beta^2 r_i - b^2 r_i - 2b) e^{-\beta r_i} \}, \quad (13)$$

where $b = 1/r_0$, $\alpha = A/4\pi$, and $\beta^2 = 4k_F/\pi a_0$. a_0 is the Bohr radius. Equation (11) is the same as given by Gubanov and Nikulin.¹⁵ Evidently the configurational energy is proportional to the effective charge of the proton.

III. RESULTS AND DISCUSSIONS

A. Configurational energy

We calculated the screened form factors

$$V_s(q) = v(q)/\Omega_0 \epsilon_0(q) \quad (14)$$

for all the metals using all the four potentials discussed in an earlier section. Ω_0 is the atomic volume. The potential parameters are tabulated in Table I, and the results are shown in Figs. 1(a)–1(c) for copper, silver, and gold, respectively.

TABLE I. Potential parameters for noble metals. All the values are in atomic units.

Potential parameters	Copper	Silver	Gold
H^a $A =$	0.465	0.425	0.514
$r_0 =$	2.42	2.73	2.72
A^b $r_0 =$	0.81	1.04	0.81
$A =$	0.5	0.68	0.50
B^c $V_0 =$	1.9	2.95	2.66
$r_1 =$	1.0	1.0	1.00
$r_2 =$	1.815	2.38	2.60
S^d $A =$	11.1	10.5	9.25
$r_0 =$	0.257	0.17	0.15

^aReference 18.

^cReference 20.

^bReference 19.

^dReference 17.

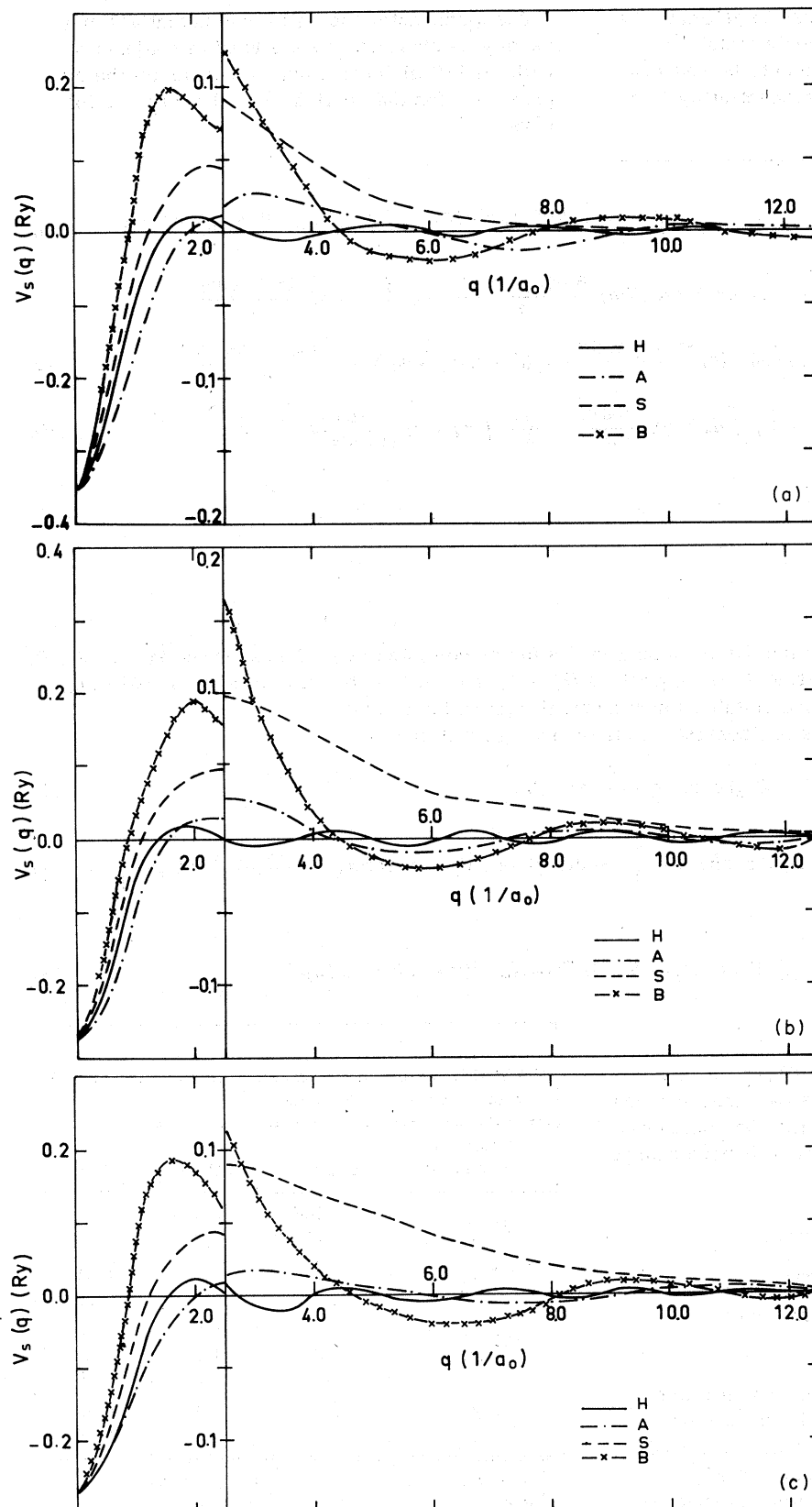


FIG. 1. (a) Screened form factors for copper. H, A, S, and B represent the Nikulin, Ashcroft, Singh and Prakash, and Borchi and De Gennaro form factors, respectively. a_0 is the Bohr radius. For $q > 2.5$, the results are shown on a magnified scale. (b) Screened form factors for silver. The description is the same as that of (a). (c) Screened form factors for gold. The description is the same as that of (a).

TABLE II. Contributions to the configurational energy of proton from nearest-neighbor host atoms when Nikulin potential and modified Hartree (MH) and Thomas-Fermi (TF) dielectric functions are used. n is the number of nearest neighbors (nn), r_1 is the distance of nn, and E_i is the corresponding contribution in rydbergs. a_1 is lattice parameter.

n	r_1	Copper		E_i (Ry) Silver		Gold	
		MH	TF	MH	TF	MH	TF
6	$\frac{1}{2}a_1$	0.2613	0.2420	0.1808	0.1748	0.0578	0.0953
8	$\frac{1}{2}a_1\sqrt{3}$	-0.0027	0.0172	-0.0062	0.0106	-0.0086	0.0058
24	$\frac{1}{2}a_1\sqrt{5}$	-0.0035	0.0078	-0.0030	0.0044	-0.0026	0.0024
30	$\frac{3}{2}a_1$	0.0007	0.0006	0.0006	0.0002	0.0006	0.0002
21	$\frac{1}{2}a_1\sqrt{11}$	0.0019	0.0001	0.00001	0.0000	-0.0003	0.0000
24	$\frac{1}{2}a_1\sqrt{13}$	0.0000	0.0000	0.0000	0.0000	-0.0004	0.0000

Nikulin form factors have the smallest wavelength and amplitude. Borchhi *et al.* form factors have the maximum amplitude, and Singh *et al.* form factors have the maximum wavelength for oscillations. Such an oscillatory behavior is not expected in TF screening limit. Therefore, the nearest neighbor (nn) contributions to the configurational energy will be decreasing exponentially while the TF screening function is used, and these will be oscillatory while the MH dielectric function is used. This is evident from the results tabulated in Table II. In the former case, the contribution from the second and third nn is of the order of 10% of the first nn and therefore not negligible. In the later case, the first nn have the repulsive interaction and second and third nn have the attractive interaction. The strength of these interactions goes on decreasing, and the major contribution is due to the first nn's. A similar effect may also arise from the lattice deformation.

The results for the configurational energy of proton in octahedral (O), tetrahedral (T), and vacant positions are tabulated in Table III. The following comments are drawn. (i) The configurational energy depends upon the position of the proton, the dielectric function, and the pseudopotential used. (ii) The Ashcroft model potential gives the lowest and the Borchhi *et al.* model potential gives the highest configurational energies for Cu and Ag, while MH and TF dielectric functions are used. The Nikulin model potential gives the lowest configurational energy for gold. (iii) Nikulin, Ashcroft, and Singh *et al.* potentials give higher configurational energies in the octahedral (O) position when TF screening function is used as compared to that when MH dielectric function is used. The trend is reversed with Borchhi *et al.* potential. No definite trend is found in the configurational energy for the T position as the proton is nearer to the host atom. (ii) The configurational energy in the

TABLE III. Configurational energy of copper, silver, and gold in Ry units. The description is the same as in Tables I and II. O (octahedral) T (tetrahedral); V (vacancy).

Potential	Position	Copper		Silver		Gold	
		MH	TF	MH	TF	MH	TF
H	O	0.2578	0.2676	0.1724	0.1900	0.0465	0.1038
	T	0.3420	0.3292	0.2473	0.2389	0.1181	0.1305
	V	0.0283	0.0966	-0.0017	0.0637	-0.0829	0.0341
A	O	0.1470	0.1946	0.1162	0.1547	0.0777	0.1359
	T	0.2229	0.2396	0.1866	0.1949	0.1433	0.1711
	V	0.0111	0.0708	-0.0064	0.0518	-0.0111	0.0456
B	O	0.4609	0.3712	0.1794	0.1646	0.2925	0.2354
	T	0.5678	0.4571	0.2735	0.2073	0.3919	0.2964
	V	0.0577	0.1350	-0.0409	0.0551	-0.0117	0.0791
S	O	0.3009	0.2834	0.1690	0.1998	0.1528	0.1724
	T	0.3928	0.3488	0.2478	0.2266	0.2298	0.2170
	V	0.0348	0.1027	-0.0075	0.0602	-0.0081	0.0579

O position is always found lower than in the T position, therefore, O position may be the more favorable position of the proton. (v) The configurational energy in vacancy is lower by an order of magnitude than in the O position and therefore, the proton will easily trap to a vacant position if available.

From these comments it is concluded that the most probable position of the proton is the position of minimum ionic density in the lattice and this conclusion is in agreement with the experimental informations.²³

B. Activation energy

To estimate the activation energies, we calculated the configurational energies of the proton as it moves along $\langle 111 \rangle$ ($O-T$) and $\langle 110 \rangle$ ($O-O$) directions. The results of these calculations are shown in Fig. 2 for copper. The solid lines represent the calculations with the MH dielectric function and the dash-dot line represents the calculations when the Ashcroft model potential in conjunction with the TF screening function is used. The qualitative behavior of the variation of the configurational energy is found to be the same for all the potentials also for silver and gold and therefore these are not shown in Fig. 2. The activation energies are calculated as the height of the energy barriers between the O and T positions, and these are tabulated in Table IV. The activation energies for A , H , S , and B potentials are in increasing order. The difference in activation energies for A and B potentials is about 40% and this is consistent with the magnitude of the form factors

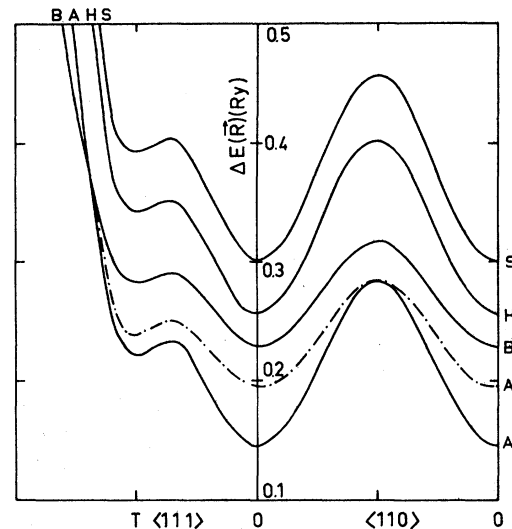


FIG. 2. Configurational energies for proton in copper. A, H, S, and B have the same description as in Fig. (1a). The solid lines are for modified Hartree dielectric screening and the dash-dot line is for Thomas-Fermi screening. Line B is on a scale reduced by a factor of 2.

shown in Fig. 1.

Along $\langle 110 \rangle$ direction, the configurational energy goes on increasing as the proton moves from the octahedral position and it is maximum between two octahedral positions. But this does not remain true while the proton moves from the octahedral to tetrahedral position. The maxima is at about 65% distance from the octahedral position. Beyond tetrahedral position, as the proton moves

TABLE IV. Activation energies for noble metals in Ry units. Z_e is the effective charge of proton. The description is the same as that of Table I. A (TF) represent the results when TF screening function is used with an Ashcroft potential.

Metal	Potential	Z_e					Expt.
		1.0	0.20	0.25	0.30	0.35	
Cu	A	0.0864	0.0173	0.0216	0.0259	0.0302	
	A (TF)	0.0554					
	H	0.0958	0.0192	0.0240	0.0287	0.0335	0.029
	S	0.1012	0.0202	0.0253	0.0304	0.0354	
	B	0.1110	0.0222	0.0278	0.0333	0.0389	
Ag	A	0.0810	0.0162	0.0203	0.0243	0.0284	
	A (TF)	0.0492					
	H	0.0838	0.0168	0.0210	0.0251	0.0293	0.024
	S	0.0890	0.0178	0.0223	0.0267	0.0312	
	B	0.1146	0.0229	0.0287	0.0344	0.0401	
Au	A	0.0760	0.0152	0.0190	0.0228	0.0266	
	A (TF)	0.0442					
	H	0.0834	0.0167	0.0209	0.0250	0.0292	0.018
	S	0.0872	0.0174	0.0218	0.0262	0.0305	
	B	0.1156	0.0231	0.0289	0.0347	0.0405	

towards the host atom, the height of the barrier increases rapidly. The energy barrier between octahedral sites is about 50% larger and wider than between O and T sites. Therefore the proton is more likely to follow the O - T - O path rather than O - O path. TF screening also gives similar results, but the activation energies are lower than in the case of MH screening. Therefore, protons may diffuse faster in a strongly screened system as the interaction becomes weaker.

We also calculated the activation energies varying the effective charge of the proton, using all the potentials and modified Hartree dielectric function. These results are also tabulated in Table IV. The calculated activation energies are in reasonably good agreement with experimental values for $Z = 0.31, 0.29,$ and 0.23 in copper, silver, and gold, respectively, using all the potentials. Borch *et al.* potential yields 15% to 20% higher results. Therefore hydrogen may be expected between the protonic and the atomic state in noble metals and a quasibound state may exist in the bottom of the conduction band. The schematic diagram for $N(E)$, the density of states, may be drawn as in Fig. 3 where $n = 3, 4, 5$ for copper, silver, and gold, respectively. Our results are in agreement with the conclusions drawn by Friedel³ in a self-consistent calculation. The effective charge on the proton decreases as the core radii increase. However, this will also depend upon the number of conduction electrons per atom available. Popovic *et al.*⁶ pointed out that the linear screening theory overestimates the activation energy of proton in Al. However, if the effective charge of the proton is taken about $0.30e$, their calculated activation energy in linear screening theory becomes in reasonably good agreement with the experimental values. Their self-consistent nonlinear calculations give a big pileup of charge around the proton and therefore the effective charge reduces. Mainwood and Stoneham¹¹ reported that hydrogen is between atomic and anionic state in bcc alkali metals. However, their cluster of 15 to 20 atoms may possibly be too small for a very realistic representation of a metallic system. Thomas-Fermi screening

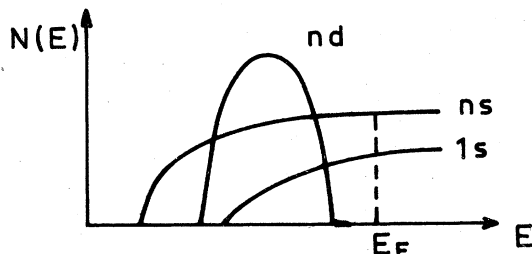


FIG. 3. Schematic diagram for density of states of metal-hydrogen system.

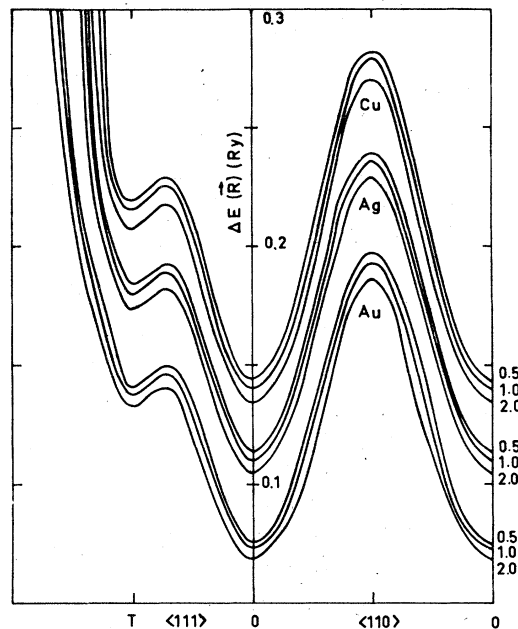


FIG. 4. Configurational energies of protons in noble metals for an expanded lattice. Ashcroft potential and modified Hartree dielectric function are used.

gives the effective charge of proton about $0.52e$, $0.49e$, and $0.41e$ in Cu, Ag, and Au, respectively, to have an agreement of activation energies with the experimental values. This is because of the overscreening in the host lattice.

Finally the movement of the proton is studied using the Ashcroft model potential and the MH dielectric function, increasing the lattice parameter by 0.5%, 1%, and 2%. The last one is approximately equivalent to the melting of the metal. The corresponding contraction in Fermi momentum is taken into account consistently. These results are shown in Fig. 4 for all the metals. Correspondingly, the activation energies decrease by 1%, 2%, and 4%, but the path of movement remains the same. This is consistent with the experimental information.²⁴

IV. CONCLUSIONS

The diffusion of a proton in noble metals is investigated using linear screening and local pseudopotential approximations. All the pseudopotentials which explain other physical properties of these metals also yield the lower configurational energy for the octahedral position of the proton in fcc lattice. However, if a vacant site is available, a proton is most likely to be trapped. The activation energies are found in reasonably good agreement with the experimental values using all the potentials if the effective charge of the proton is taken $0.31e$, $0.29e$, and $0.23e$ in copper, silver,

and gold, respectively. The activation energies are found to decrease as the lattice expands.

ACKNOWLEDGMENTS

The author expresses his sincere thanks to Professor P. Lucasson and Professor J. Friedel

for invaluable discussions and continuous encouragement, and to the members of Bourse Juliot Curie committee for the grant. He is grateful to Professor A. Lucasson for her kind hospitality and acknowledges the informative discussions with Dr. J. Daou and Dr. J. Bonnet.

*Permanent address: Physics Dept., Panjab University, Chandigarh, India.

¹Ber. Bunsenges. Phys. Chem. 76, No. 8 (1972).

²*Hydrogen in Metals*, edited by I. R. Harris, and J. P. G. Farr, (Elsevier Sequoia, Lausanne, 1976).

³J. Friedel, *Philos. Mag.* 43, 153 (1952); *Ber. Bunsenges. Phys. Chem.* 76, 828 (1972).

⁴P. Leonard, *J. Phys.* 28, 328 (1967).

⁵Z. D. Popovic and M. J. Stott, *Phys. Rev. Lett.* 33, 1164 (1974).

⁶Z. D. Popovic, M. J. Stott, J. P. Carbotte, and G. R. Piercy, *Phys. Rev. B* 13, 590 (1976).

⁷J. P. Carbotte, *Phys. Rev.* 155, 197 (1967).

⁸C. D. Gelatt, J. A. Weiss, and H. Ehrenreich, *Solid State Commun.* 17, 663 (1975).

⁹C. P. Flynn and A. M. Stoneham, *Phys. Rev. B* 1, 3966 (1971).

¹⁰A. M. Stoneham, *J. Phys. F* 2, 417 (1972).

¹¹A. M. Mainwood and A. M. Stoneham, *J. Less Common Met.* 49, 271 (1976).

¹²H. K. Birnbaum and C. P. Flynn, *Phys. Rev. Lett.* 37, 25 (1976).

¹³D. Lepski, *Phys. Status Solidi* 35, 697 (1969).

¹⁴E. Gorham-Bergeron, *Phys. Rev. Lett.* 37, 146 (1976).

¹⁵A. I. Gubanov and V. K. Nikulin, *Sov. Phys.-Solid State* 7, 2184 (1966).

¹⁶P. Vashishta and K. S. Singwi, *Phys. Rev. B* 6, 875 (1972).

¹⁷N. Singh and S. Prakash, *Phys. Rev. B* 8, 5532 (1973);

10, 2652 (1974); R. Prasad, S. Auluck, and S. K. Joshi, *J. Phys. F* 5, 1385 (1975).

¹⁸V. K. Nikulin, *Sov. Phys.-Solid State* 7, 2189 (1965).

¹⁹N. W. Ashcroft and D. C. Langreth, *Phys. Rev.* 155, 682 (1967).

²⁰E. Borchi and S. De Gennaro, *Phys. Lett. A* 34, 19 (1971).

²¹V. K. Nikulin, *Phys. Lett. A* 36, 337 (1971), and references therein.

²²E. Borchi and S. De Gennaro, *Phys. Rev. B* 5, 4761 (1972).

²³A. Lucasson, P. Lucasson, and G. Budin, *J. Phys.* 25, 571 (1964); 25, 1004 (1964).

²⁴A. B. McLellan, *J. Phys. Chem. Solids* 34, 1137 (1973).